Received: 21 November 2017 | Revised: 13 March 2018 | Accepted: 4 March 2018

DOI: 10.1002/kin.21178

ARTICLE

WILEY

Reactivity of *cis*-platinum(II) complexes with 2-(4-substituted)phenylthiomethyl)quinoline nonleaving ligands toward thiourea nucleophiles

Wakhiwe M. Mthiyane | Allen Mambanda | Deogratius Jaganyi

School of Chemistry and Physics, University of KwaZulu-Natal, Scottsville, South Africa

Correspondence
Allen Mambanda, School of Chemistry and Physics, University of KwaZulu-Natal, Scottsville, 3209, South Africa.
Email: mambanda@ukzn.ac.za

Abstract

The sequential substitution of aqua ligands from [Pt{2-(phenylthiomethyl)quinoline}$(H_2O)_2$]CF_3SO_3, **Pt(L1)**, [Pt{2-(4-*tert*-butylphenylthiomethyl)quinoline}$(H_2O)_2$]CF_3SO_3 **Pt(L2)**, and [Pt{2-(4-fluorophenylthiomethyl)quinoline}$(H_2O)_2$]CF_3SO_3 **Pt(L3)** by thiourea nucleophiles (Nu) was studied under pseudo–first-order conditions as a function of concentration and temperature using stopped-flow and UV-visible spectrophotometric techniques. The observed pseudo–first-order rate constants for the substitutions can be described by the rate law: $k_{obs(1/2)} = k_{2(1/2)}$[Nu], where the subscript denotes the consecutive substitution steps. The first aqua ligand was substituted opposite to the strong σ-trans-directing thioether followed by the aqua ligand opposite to the quinoline or pyridine moieties. Second-order rate constants, $k_{2(1st)}$, for the substitution of the first aqua ligand by thiourea nucleophiles ranged between 9 and 22 M^{-1} s^{-1} for **Pt(L1),** 86 and 326 M^{-1} s^{-1} for **Pt(L2),** and 58 –287 M^{-1} s^{-1} for **Pt(L3)**. The ranges of the second-order rate constant, $k_{2(2nd)}$, were always lower than the $k_{2(1st)}$'s and are 0.3-9 M^{-1} s^{-1} for **Pt(L1),** 2-20 M^{-1} s^{-1} for **Pt(L2),** and 0.3-5 M^{-1} s^{-1} for **Pt(L3)**. Aqua substitution from **Pt(L2)** is slower for both steps than from **Pt4**, its pyridyl derivative from our previous study. A Job's method of continuous variation plot suggests a species with a metal-to-nucleophile ratio of 1:3 as the ultimate product of the chloride substitution from the Pt(II) complexes by the incoming thiourea nucleophiles. The high and negative activation entropy and low and positive activation enthalpy values support an associative mechanism of activation, characteristic of substitution reactions occurring in square-planar complexes.

KEYWORDS

associative mechanism, consecutive reaction, Pt(II) mononuclear complexes, substitution

1 | INTRODUCTION

Square-planar Pt(II) complexes have been a subject of medicinal interest for years.[1,2] The reactions of these complexes with DNA nucleic bases provide one of the many mechanistic pathways for anticancer activity against cancerous cells.[3] Modification of both steric and electronic attributes of the nonleaving ligand is key to adjusting the reactivity of Pt(II) complexes required to optimize their antitumur potency.[4] For example, despite the high reactivity of the square-planar Pd(II) complexes (factors of between 10^3 and 10^5 over their Pt(II) analogues), there are several Pd(II)complexes which have shown comparable in vitroantitumur activity[5]. Highly reactive Pt(II)/Pd(II) complexes would rapidly hydrolyze and be deactivated by nontargeted substrates in the plasmic fluids.[6] This also leads to high toxicity and development of

resistance.[7] It can therefore be hypothesized that nonactive anticancer Pd(II) compounds become active agents if their reactivity can be reduced to levels commonly reported for Pt(II) complexes. Possibilities include introducing sterically bulky nonleaving ligands that retards a facile approach of other extracellular bionucleophiles[8] or ligands that are stronger σ-donors but weaker π-acceptors.

An important subgroup of square-planar Pt(II) complexes has been those which possess two sites for substitution. The remaining sites are occupied by two monodentates or a bidentate ligand. Examples are Pt(II) complexes, which have N,N-[8–13] or N,S-[14,15] bidentate nonleaving ligands and these usually display a two-step consecutive substitution of the labile leaving groups, with rates that are dependent on the electronic (σ-donor/π-acceptor) and steric demands of the resident ligand as well as the nucleophilicity of the labile ligands. Even in complexes where the coordinated bidentate ligand is symmetrical, substitution occurred consecutively.[16] A case in point is the chloride substitution from the Pt(II) complex Pt(1,2-bis(phenylsulfanyl)ethane)Cl_2 (S,S = 1,2-bis(phenylsulfanyl)ethane) by pyridine.[17] Substitution of the first chloride ligand is followed by a ring opening of the S,S ligand.

When the nonleaving ligand has fused aromatic rings, the rate of substitution of square-planar Pt(II) complexes is increased due to the strong π-acceptor property of the ligand. In principle, extending the π-surface of a strong π-acceptor ring such as pyridine to a quinoline moiety is expected to accelerate the rate of substitution due to an increased propensity of the latter moiety to receive electron density into its lower energy, extended molecular orbitals. However, recent reports[18,19] have demonstrated an antithesis of this observation. Relative to the reactivity of Pt(II)(terpy)Cl, terpy = 2,2′:6-terpyridine, Pt(II) complexes bearing 2,6-bis(iso/quinolyl)pyridine have been found to have surprisingly lower rates of substitution.[19] A stronger σ-effect and poor π-acceptor properties of the iso/quinolyl groups have been put forward to explain this anomaly. As a result, electron density is accumulated on the bis(iso/quinolyl)pyridine Pt(II) complexes relative to that of Pt(II)(terpy)Cl, leading to a more destabilized transition state in the former complexes.[20,21] A similar trend in reactivity was observed by Khusi et al.[22] for N,N bidentate coordinated Pt(II) complexes for which replacing the pyridyl moiety of the bidentate with a quinolyl moiety retarded the rate of stepwise substitution of the aqua leaving groups positioned trans to the moiety.

This study extends the knowledge on the role of quinolyl nonleaving ligand on the rate of aqua ligand substitution in *cis*-Pt(II) complexes bearing 2-(4-substituted) phenylthiomethyl)quinoline (N,S) bidentate ligands (Figure 1). The entering thiourea nucleophiles were chosen due to their neutral character, good aqueous solubility, and nucleophilicity.[23]

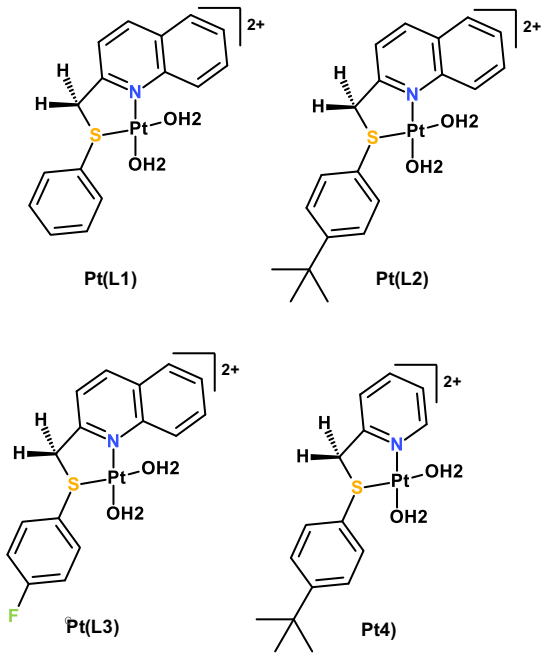

FIGURE 1 Structures of the *cis*-Pt(II) complexes with 2-(phenylthiomethyl)quinoline moieties [Color figure can be viewed at wileyonlinelibrary.com]

2 | EXPERIMENTAL

2.1 | Materials

Chemicals and solvents (analytical grade or better) were all purchased from Aldrich and Merck (Johannesburg, South Africa), respectively, and used without further purification. Silver trifluoromethanesulfonate ($AgCF_3SO_3$; 99%; Aldrich) was stored under nitrogen as per specifications. Ultrapure water (MODULAB purification system) was used for all aqueous solutions.

2.2 | Synthesis of the N, S ligands

Synthesis of the ligands was carried out under inert conditions using standard Schlenk techniques. Bidentate N,S ligands, namely 2-(phenylthiomethyl)quinoline (**L1**), 2-(4-*tert*-butylphenylthiomethyl)quinoline (**L2**), and 2-(4-fluorophenylthiomethyl)quinoline (**L3**), were prepared via a nucleophilic S-alkylation reaction of either thiophenol (0.62 mL, 6.8 mmol), 4-*tert*-butylthiophenol (1.20 mL, 6.9 mmol), or 4-fluorothiophenol (0.70 mL, 6.8 mmol) with 2-(chloromethyl)quinoline hydrochloride (1.5 g, 6.8 mmol) under basic conditions.[24,25] 2-(Chloromethyl)quinoline hydrochloride was dissolved in water (3 mL). To the stirring solution, 5 M NaOH was added drop by drop until a pink emulsion was observed. A solution of the thiophenol in absolute EtOH (10 mL) was added dropwise. The mixture was stirred under reflux for 36 h. Upon cooling, the product was sequentially extracted with $CHCl_3$ (4 × 10 mL). The

combined organic phases were back-washed with 2 × 10 mL portions of cold ultrapure water. Yellow or orange brown oils (yield: 58-64%) of adequate purity for further use for platinum coordination were obtained after solvent removal under vacuum. Suitable crystals for X-ray analysis of **L1** and **L3** were obtained by slow vapor diffusion of hexane into concentrated dichloromethane solutions of their oils.

2.2.1 | Spectroscopic characterisation

L1: Yield: 1.07 g, 4.3 mmol (63%, brown orange oil). ^{1}H NMR (400 MHz: $CDCl_3$): δ_H (ppm) referenced to TMS; 4.47 (s, 2H, –CH_2–), 7.16-7.20 (t, 1H, Ph), 7.24-7.27 (t, 2H, Ph), 7.40-7.42 (d, 2H, Ph), 7.52-7.56 (d, 1H, Qn), 7.52-7.56 (t, 1H, Qn), 7.71-7.75 (t, 1H, Qn), 7.80-7.82 (d, 1H, Qn), 8.07 (d, 1H, Qn), 8.13 (d, 1H, Qn). ^{13}C NMR (100 MHz: $CDCl_3$): δ_C (ppm); 41.1; 120.9; 126.4; 127.1; 127.5; 128.9; 129.1; 129.7; 136.9; 158.1. Infrared (KBr, 4000-650 cm^{-1}) ν: 3056 (C=C–H asymmetric stretch), 1596 (C=N, quinolyl). Time-of-flight MS-ESI$^+$ *m/z*: 252.0961, 100 $(M)^+$. Anal. Calcd for $C_{16}H_{13}NS$: C: 76.46, H: 5.21, N: 5.57, S: 12.76. Found: C: 76.31, H: 5.25, N: 5.21, S: 12.51.

L2: Yield: 1.24 g, 4.0 mmol (58%, orange oil). ^{1}H NMR (400 MHz: $CDCl_3$): δ_H (ppm) referenced to TMS; 1.30 (s, 9H, –$C(CH_3)_3$), 4.45 (s, 2H, –CH_2–), 7.27 (d, 2H, Ph) 7.35 (d, 2H, Ph) 7.51 (t,1H, Qn), 7.56 (d, 1H, Qn), 7.70-7.74 (t, 1H, Qn), 7.79-7.81 (d, 1H, Qn), 8.08 (d, 1H, Qn), 8.10-8.12 (d, 1H, Qn). ^{13}C NMR (100 MHz: $CDCl_3$): δ_C (ppm); 41.8; 115.8; 116.1; 122.1; 123.1; 130.3854; 133.1091; 136.6; 149.3; 157.6. Infrared (KBr, 4000-650 cm^{-1}) ν: 3059 (C=C–H Asymmetric stretch), 1598 (C=N, quinolyl). Anal. Calcd for $C_{20}H_{21}NS$: C: 78.13, H: 6.88, N: 4.56, S: 10.43. Found: C: 78.01, H: 6.62, N: 4.53, S: 10.84.

L3: Yield: 1.14 g, 4.2 mmol (64%, orange oil). ^{1}H NMR (400 MHz: $CDCl_3$): δ_H (ppm) referenced to TMS; 4.40 (s, 2H, –CH_2–), 6.92-6-.96 (d, 2H, Ph), 7.34-7.38 (d,2H, Ph), 7.47–7.49 (d, 1H, Qn), 7.52-7.56 (t, 1H, Qn), 7.70-7.74 (t, 1H, Qn), 7.79-7.81 (d, 1H, Qn), 8.05 (d, 1H, Qn), 8.11 (d, 1H, Qn). ^{13}C NMR (100 MHz: $CDCl_3$): δ_C (ppm); 42.3; 115.9; 116.1; 11.0; 126.5; 127.5; 129.8; 131.3; 133.1; 158.0. Infrared (KBr, 4000-650 cm^{-1}) ν: 3057 (C=C–H asymmetric stretch), 1592 (C=N, quinolyl). Time-of-flight MS-ESI$^+$ *m/z*: 268, 100 (M-1). Anal. Calcd for $C_{16}H_{12}FNS$: C: 71.35, H: 4.49, N: 5.20, S: 11.91. Found: C: 71.29, H: 4.31, N: 5.15, S: 11.43.

2.3 | Synthesis of Pt(II) complexes

Three mononuclear *cis*-Pt(II) complexes, *viz.* [Pt{2-(phenylthiomethyl)quinoline}Cl_2], **Pt(L1)Cl_2**, [Pt{2-(4-*tert*-butyl thiophenol)quinoline}Cl_2], **Pt(L2)Cl_2**, and [Pt{2-(4-fluorothiophenol)quinoline}Cl_2], **Pt(L3)Cl_2,** were synthesized by reacting 1 equiv of the respective thioether ligand with K_2PtCl_4 (0.46 g, 0.9 mmol) according to a literature method.[26]

2.4 | Spectroscopic characterisation

Pt(L1)Cl_2: Yield: 0.36 g, 0.69 mmol (77%, orange powder). ^{1}H NMR (400 MHz: DMF-d_7): δ_H (ppm) referenced to TMS; 4.30 (d, 2H, –CH_2–, AB-spin system), 7.16 (t, 1H, Ph), 7.27 (t, 2H, Ph), 7.37 (d, 2H, Ph), 7.33 (t, 1H, Qn), 7.52-7.54 (d, 1H, Qn), 7.60-7.64 (t, 1H, Qn), 8.56 (d, 1H, Qn). ^{195}Pt NMR (400 MHz: DMF-d_7): δ_{Pt} (ppm); –2717. Infrared (KBr, 4000-650 cm^{-1}) ν: 3055 (C=C–H asymmetric stretch), 1583 (C=N, quinolyl). Anal. Calcd *for* $C_{16}H_{13}Cl_2NPtS$: C: 37.15, H: 2.53, N: 2.71, S: 6.20. Found: C: 36.98, H: 2.42, N: 2.57, S: 6.02.

Pt(L2)Cl_2: Yield: 0.2 g, 0.36 mmol (60%, yellow-orange powder). ^{1}H NMR (400 MHz: $CDCl_3$): δ_H (ppm) referenced to TMS; 1.30 (s, 9H, –$C(CH_3)_3$), 4.27 (d, 2H, –CH_2–, AB-spin system), 7.17-7.18 (t, 1H, Qn), 7.28 (d, 4H, Ph), 7.36 (d, 1H, Qn), 7.62-7.65 (t, 1H, Qn), 8.55 (d, 1H, Qn). ^{195}Pt NMR (400 MHz: DMF-d_7): δ_{Pt} (ppm); –2711. Infrared (KBr, 4000-650 cm^{-1}) ν: 3059 (C=C–H asymmetric stretch), 1598 (C=N, quinolyl). Anal. Calcd *for* $C_{20}H_{21}Cl_2NPtS$: C: 41.89, H: 3.69, N: 2.44, S: 5.59. Found: C: 41.35, H: 3.30, N: 2.69, S: 5.57.

Pt(L3)Cl_2: Yield: 0.2 g, 0.37 mmol (44%, yellow-orange powder). ^{1}H NMR (400 MHz: $CDCl_3$): δ_H (ppm) referenced to TMS; 4.19 (d, 2H, –CH_2–, AB-spin system), 6.91-7.00 (d, 2H, Ph), 7.12-7.15 (t, 1H, Qn), 7.23 (d, 1H, Qn), 7.32 (d, 2H, Ph), 7.57-7.60 (t, 1H, Qn), 8.51-8.52 (d, 1H, Qn). ^{195}Pt NMR (400 MHz: DMF-d_7): δ_{Pt} (ppm); –2718. Infrared (KBr, 4000-650 cm^{-1}) ν: 3066 (C=C–H asymmetric stretch), 1588 (C=N, quinolyl). Anal. Calcd for $C_{16}H_{12}Cl_2FNPtS$: C: 35.90, H: 2.26, N: 2.62, S: 5.98. Found: C: 35.64, H: 2.05, N: 2.52, S: 6.06.

2.5 | Preparation of the diaqua Pt(II) complexes

Solutions of the diaqua complexes, viz. **Pt(L1)**, **Pt(L2),** and **Pt(L3),** were prepared from their chloride derivatives via a chloride metathesis with $AgCF_3SO_3$ followed by dilution with a pH 2 triflic acid solution.[27] Solutions of the thiourea nucleophiles, viz. **tu**, **dmtu**, and **tmtu**, were prepared by dissolving a known amount of the nucleophile in 0.1 M LiOTf/HOTf solution.

2.6 | Instrumentation and physical measurements

NMR spectrometers (Bruker Avance DRX 400 or DRX 500) and a FLASH 2000 CHNS analyzer were used for the characterization and chemical analysis of the ligands and complexes, respectively. A Waters Micromass LCT Premier mass spectrometer (ESI^+-TOF) was used to acquire mass spectra of the ligands and complexes. A Perkin Elmer Spectrum One FTIR spectrometer was used to measure the characteristic frequencies of vibration of the ligands and complexes. Rapid kinetic measurements were performed on an Applied Photophysics SX 20MV stopped-flow spectrophotometer coupled to an online data acquisition system. The temperature of the instrument was controlled to within ± 0.1°C for all measurements. A Cary 100 BIO UV-visible spectrophotometer equipped with a Varian Peltier temperature controller (with an accuracy of ±0.05°C) was used for the determination of the pK_a values of the diaqua complexes. The pH measurements were determined on a Jenway 4330 pH meter equipped with a 4.5-μm glass electrode. The micro-electrode was calibrated at 25°C using standard buffer solutions (Merck) at pH 4.0, 7.0, and 10.0. pK_a titration curves. and time-resolved kinetic traces were graphically analyzed using Origin 7.5® software package.[28]

2.7 | pK_a determination for the diaqua complexes

Spectrophotometric acid-base titrations were undertaken for the determination of pK_a values of the diaqua complexes. Changes in absorbance of the diaqua complex after addition of aliquots of NaOH were plotted as a function of pH within the range 2-9. In the low pH range (2-3), ΔpH for the titrated solution was small and thus required crushed NaOH pellets. For the subsequent increase in pH, dilute NaOH solutions of varying concentrations were used. After each addition, about 0.5 mL of the solution was sampled for pH measurement. These samples were discarded to avoid probable contamination from leached off chloride ions from the pH electrode. The pK_a values were obtained from a sigmoidal curve fitting of data.

2.8 | Kinetics measurements

The rate of substitution of the coordinated aqua ligands from the Pt(II) complexes was undertaken under pseudo–first-order conditions for which the concentration of nucleophile was at least 10-fold more than the Pt(II) complex. At all times, the solutions were kept at pH 2 to ensure the presence of only the diaqua form of the complexes in solution. The rate of slow reactions was followed on the UV-visible spectrophotometer following a manual mixing of the complex and the nucleophile in a tandem Suprasil cuvette. For rapid reactions, an automated stopped-flow analyzer equipped with a pressure-driven cross-mixer for instant mixing of the complex and nucleophile solutions was used. Prior to kinetics measurements on the stopped-flow analyzer, trial kinetic reactions of the Pt(II) metal complexes with the nucleophiles were briefly undertaken by scanning the entire UV-visible wavelength range. This was done to determine a suitable wavelength at which kinetics of each reaction could be followed. Rate constants from the UV-visible scanning kinetics of slow reactions are averages of duplicates, whereas those from the stopped-flow analyzer are averages of eight independent kinetic runs. The temperature dependence of the rate of substitution was studied within the range of 15-35°C.

2.9 | Job's method of continuous variation

The complex formation reaction of the Pt(II) complexes with the thiourea nucleophiles was studied by preparing solutions of **Pt(L2)** (0.1 mM) and **tu** (0.1 mM), adjusted to a constant ionic strength $I = 0.1$ M LiOTf/HOTf and to a pH of 2, at various mole fractions of reactants. The reaction mixtures were left for 10 h after which their absorbance was recorded at 293 nm.

2.10 | Density functional theory calculations

The geometry-optimized molecular structures of the complexes **Pt(L1)**, **Pt(L2),** and **Pt(L3)** were computed at the density functional theory (DFT) level of theory (B3LYP (CPCM)/LANL2DZp//B3LYP/-LAN2DZp)[29–31] using the Gaussian 09 software suite.[32] The geometry-optimized structures were conducted in the gaseous phase, and the calculated structural parameters along with those of **Pt4**, a pyridyl derivative of **Pt(L2)** from our previous report[33], are presented in Table 3 and Figure 4, respectively. A charge of +2 was maintained for the cationic diaqua complexes.

2.11 | X-ray crystallographic analysis

X-ray crystallographic data of the ligands **L1** and **L3** (Table 1) were collected on a Bruker Apex II Duo equipped with an Oxford Instrument Cryojet operating at 100 K and an Incoatec microsource operating at 30 W power. A Mo Kα ($\lambda = 0.71$ Å) radiation induced at a crystal-to-detector distance of 50 mm was used to collect the data. The Bruker instrument was optimized for the ω and φ scans with exposures taken at 30 W X-ray power and 0.50° frame widths using APEX2. Data reduction was done with SAINT[34] suite of program using outlier rejection, scan speed scaling, and standard Lorentz and polarization correction factors. The structure was solved and refined using SHELXS-97 and SHELXL-97 methods, respectively.[35]

TABLE 1 Crystal data of **L1** and **L3**

Parameter	L1		L3	
Empirical formula	$C_{16}H_{13}NS$		$C_{16}H_{12}FNS$	
Formula weight	251.33		269.33	
Crystal system	Triclinic		Monoclinic	
Space group	*P* -1		*P* 21/*c*	
Unit cell dimensions	$a = 7.4668(5)$ Å $b = 9.4581$ (6) Å $c = 9.9116$ (7) Å	$\alpha = 84.427(3)°$ $\beta = 76.236(2)°$ $\gamma = 70.928(4)°$	a = 28.5558(18) Å b = 5.8129(4) Å c = 7.7442(15) Å	$\alpha = 90°$ $\beta = 95.078(2)°$ $\gamma = 90°$
Volume	642.41 (8) $Å^3$		1280.43(15) $Å^3$	
Z	2		4	
Density (calculated)	1.299 mg/m^3		1.397 mg/m^3	
Absorption coefficient	0.232 mm^{-1}		0.248 mm^{-1}	
Reflections collected	2790		20940	
Independent reflections	2790		3130 [*R*(int) = 0.0192]	
Goodness-of-fit on F^2	1.092		1.084	
Final *R* indices [$I > 2\sigma(I)$]	$R_1 = 0.0434$, $wR_2 = 0.1308$		$R_1 = 0.0371$, $wR_2 = 0.0944$	
R indices (all data)	$R_1 = 0.0452$, $wR_2 = 0.1337$		$R_1 = 0.0386$, $wR_2 = 0.0952$	
Largest difference peak and hole	0.428 and –0.352 e $Å^{-3}$		0.693 and –0.352 e $Å^{-3}$	

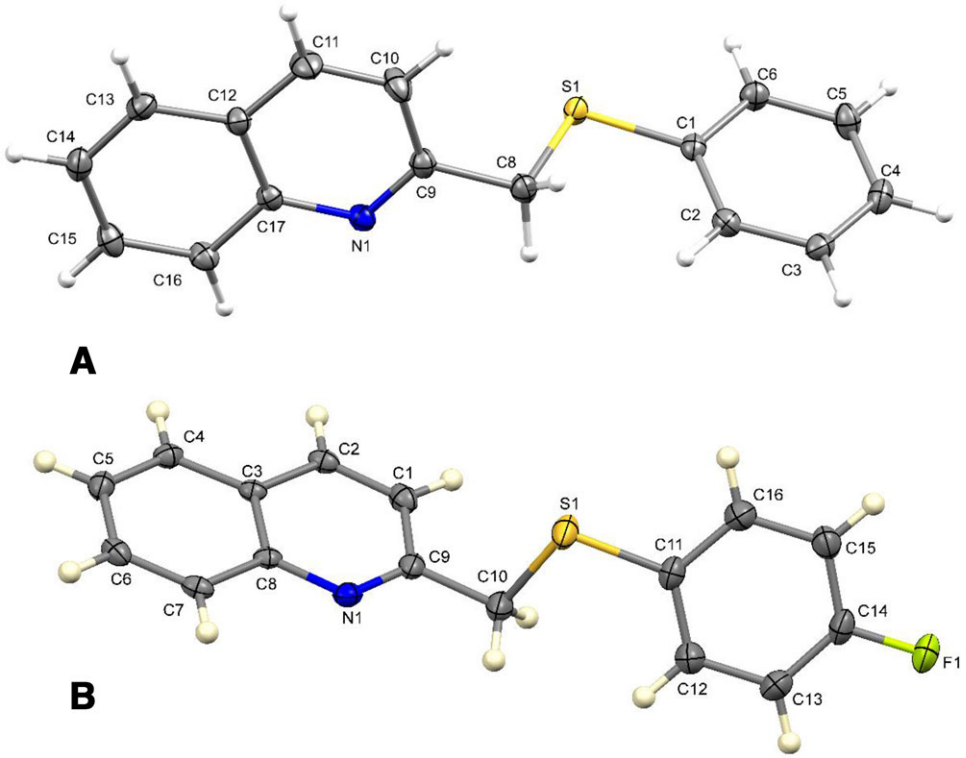

FIGURE 2 Ortep structures of **L1** (A) and **L3** (B) drawn at 50% probability ellipsoids [Color figure can be viewed at wileyonlinelibrary.com]

The ligand **L1** crystallized in the triclinic space group (with $Z = 2$), whereas **L3** crystallized in the monoclinic space group *P*21/*c* (with $Z = 4$). Their crystal structures are shown in Figure 2, and a summary of their crystal data and structure refinement details are summarized in Table 4.

3 | RESULTS

3.1 | X-ray diffraction data of ligands: L1 and L3

Figures 2 shows the crystal structures of the quinolyl N,S bidentate ligands **L1** (A) and **L1** (B).

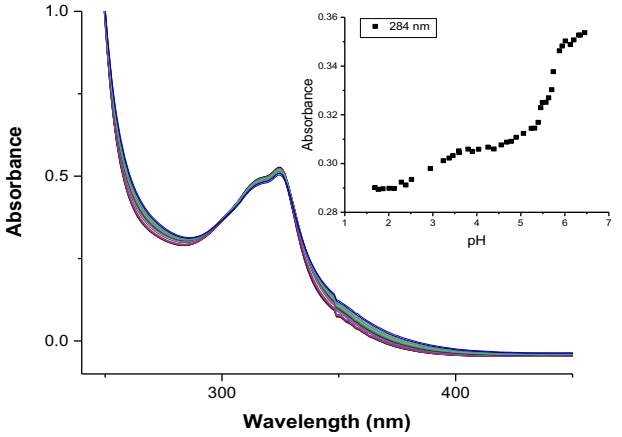

FIGURE 3 UV-visible spectra for the titration of 0.2 mM **Pt(L1)** with NaOH in the pH range 2-7 at $T = 298$ K. Inset: Absorbance versus pH data at 284 nm [Color figure can be viewed at wileyonlinelibrary.com]

TABLE 2 pK_a values of the diaqua Pt(II) complexes

	Pt(L1)	Pt(L2)	Pt(L3)	Pt4
pK_{a1}	3.95 ± 0.04	4.12 ± 0.01	4.00 ± 0.02	3.87 ± 0.04[a]
pK_{a2}	5.85 ± 0.02	6.10 ± 0.05	5.67 ± 0.03	5.60 ± 0.06[a]

[a]pK_a values reproduced from Mthiyane et al.[33]

In the crystal structures of both the ligands, coordination atoms N_1 and S_1 are spaced out by a flexible methylene carbon and have an anticonformation. This conformation minimizes electron-electron repulsions caused by the lone pairs on these atoms in the packing. For coordination on the Pt metal center to occur, the quinolyl and thioether groups must rotate about the C_8-C_9 (**L1**) or C_9-C_{10} (**L3**) bond. The acute angle (optimal arrangement of two groups and two lone pairs of electrons around S) made by the quinolyl and thioether groups is significantly lower (showing more localization of the electron density of the lone pairs around S) for the **L1** compared to its substituted analogue **L3**, in agreement with the negative inductive effect of the fluoro substituent in the latter ligand.

3.2 | Acidity of the diaqua Pt(II) complexes

Figure 3 shows an example of the spectral changes observed during the spectrophotometric titration of **Pt(L1)** with NaOH.

The pK_a values were calculated from separate single sigmoidal curve fitting (not shown in the figure) of changes in absorbance data using the Boltzmann distribution parameters as shown from the inset in Figure 3 for complex **Pt(L1)**. The values are summarized in Table 2 along with those of **Pt4**.[33]

The acid-base neutralization reaction is a consecutive two-step reaction process, wherein [Pt(N,S)(H_2O)(OH)] is an intermediate and is summarized in Scheme 1. The pK_a values of the **Pt4** was included for comparison with its quinolyl analogue.

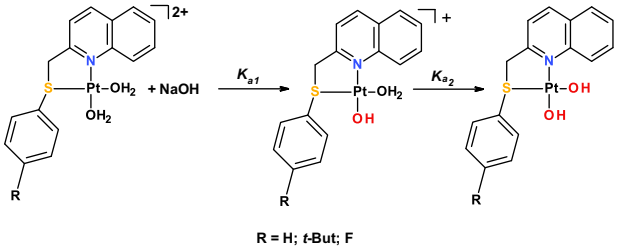

Scheme 1. Deprotonation of the diaqua Pt(II) complexes [Color figure can be viewed at wileyonlinelibrary.com]

The results in Table 2 show the sensitivity of the pK_a values due to the differences in the electronic effects of the substituents on the phenyl para-position of the N,S ligand. The pK_{a1} values for the deprotonation of the first coordinated aqua ligand increase in the order: **Pt4 < Pt(L3) < Pt(L1) < Pt(L2)**, respectively. The positive σ-inductive effect of the *tert*-butyl group causes accumulation of electron density on the Pt(II) metal center for **Pt(L2)**. This makes the Pt atom less electrophilic and the formation of the aqua-hydroxo species from the diaqua kinetically unfavorable due to a weaker Pt–OH_2 bond. This in turn makes deprotonation of the aqua ligand more difficult. Consequently, a higher pK_{a1} value is observed for **Pt(L2)** when compared to **Pt(L1)**, which only has a weaker σ-donor phenyl ring.

Owing to the negative σ-inductive effect of the fluoro substituent, electron density is withdrawn from the phenylthioether group, making the Pt atom more electrophilic in **Pt(L3)**. Hence, it can stabilize more efficiently the hydroxo species, which forms during the neutralization process. The trend in the pK_a from this study is the same as that reported by Khusi et al.[22] for similar Pt(II) complexes bearing N,N bidentate ligands. The complex bearing electron-withdrawing groups (–CF_3) on the 3,5-positions of the pyrazole ring had a lower pK_a of 4.07 when compared to a pK_a of 4.88 for the analogous complex with electron-donating methyl substituents (–CH_3).

The smaller pK_a values for the complex **Pt4** when compared to its quinolyl analogue **Pt(L2)** is due to the difference in π-acceptor properties of the nonleaving ligands. Relative to the quinolyl group of **Pt(L2)**, the pyridyl group of **Pt4** is a superior π-acceptor of electron density from the Pt(II) orbitals and thus stabilizes the hydroxo intermediate better.[14] As a result, deprotonation of the first aqua ligand occurs at lower pK_{a1} values for **Pt4** when compared to its quinolyl derivative.

3.3 | Density functional theory–calculated structures

The three Pt(II) complexes all have a common quinolyl moiety in the bidentate N,S nonleaving ligand and only differ in the substituents in the phenyl ring of the thioether group.

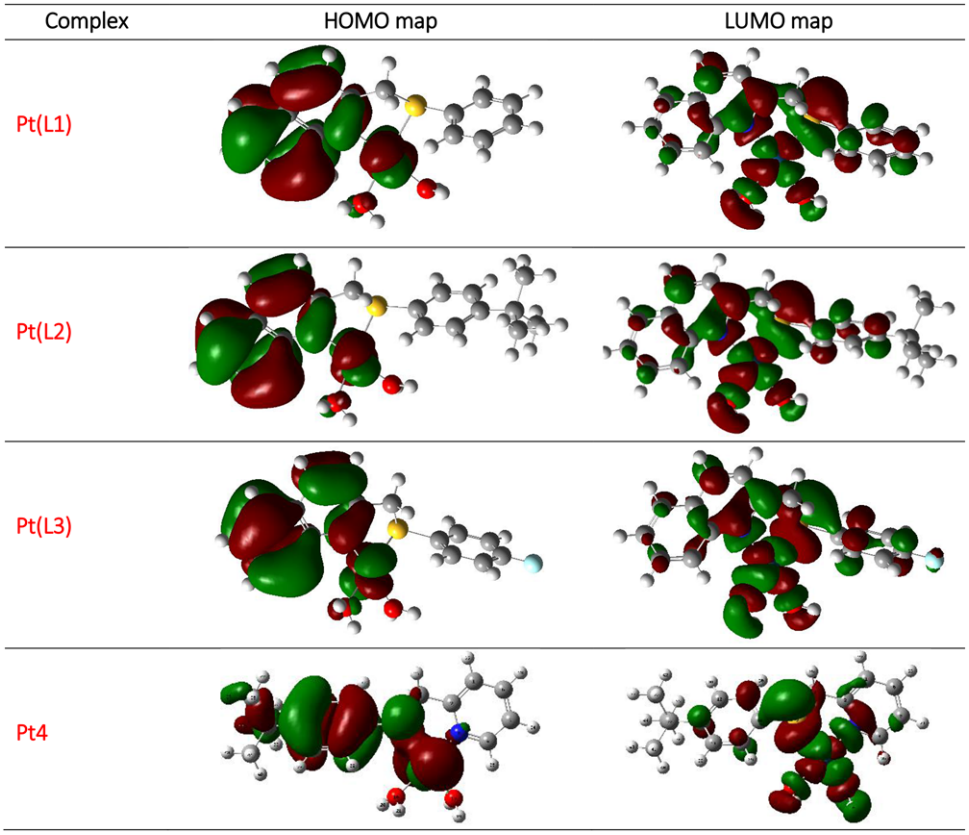

FIGURE 4 DFT geometry-optimized structures of the Pt(II) complexes [Color figure can be viewed at wileyonlinelibrary.com]

DFT calculations were performed to compare the structural parameters related to the subtle differences on the substituents on the phenyl ring of the thioether group. The coordination of the N,S-bidentate ligands to Pt is similar to that of Pt(II) complexes previously reported.[19,22,36] Geometry-optimized structures and the highest molecular orbital (HOMO) and lowest molecular orbital (LUMO) frontier molecular orbitals are depicted in Figure 4, whereas the molecular geometry–optimized parameters are summarized in Table 3. Bond angles indicate a slightly distorted square-planar around the Pt(II) metal center.

For the quinoline complexes, a significant isodensity of the HOMOs lies on the quinoline moiety. The HOMOs are also located on the Pt(II) metal center but at a much lower density. A larger isodensity mapping of the HOMOs on the N,S bidentates of quinolyl complexes projects a less electrophilic Pt (II) ion when compared to their pyridyl analogues. The LUMOs are concentrated on the thioether and to a lesser extent on the quinoline moiety. A larger LUMO mapping of electron density on the thioether indicates a poor π-acceptor capacity of this moiety and its propensity to accept electronic charge from the metal center, making the latter more electropositive. There is no significant difference in the energy gaps, $\Delta E_{\text{(HOMO-LUMO)}}$ of the frontier orbitals, although the strong electron-donating *tert*-butyl moiety for **Pt(L2)** increases the gap slightly when compared to the weak σ-donor phenyl for **Pt(L1)** and the electron-withdrawing fluoro for **Pt(L3)** substituents. The nonbonding orbital (NBO) charges (Table 3) increase in the following order: **Pt4** (0.641) < **Pt(L1)** (0.645) < **Pt(L3)** (0.648) < **Pt(L2)** (0.676) and reflects the strength of π-backbonding capacity of the ligands. A comparison of the NBO values of **Pt(L2)** relative to **Pt4** attests that stronger π-acceptor pyridine ring makes the Pt atom of **Pt4** more electrophilic.[37,38]

In addition, the electrophilicity indices (ω) increase in the order: **Pt(L3)** (7.06) < **Pt(L1)** (6.97) < **Pt(L2)** (6.85) < **Pt4** (6.48), indicating the lesser tendency of **Pt(L2)** to accepting electronic charge when compared to **Pt(L3)**. Through positive inductive donation of electron density into the thiophenyl group, the *tert*-butyl group of the former complex makes the Pt atom less electrophilic whereas the fluoro group of **Pt(L3)** withdraws electronic charge from the Pt atom inductively.

3.4 | Kinetic measurements

Substitution of the aqua coligands from the Pt(II) complexes by thiourea nucleophiles proceeds by a two-step sequential process represented by $k_{2(1st)}$ and $k_{2(2nd)}$ as depicted in Scheme 2. The mechanism of substitution is similar to what has been reported for the reactions of pyridyl derivatives of these complexes.

TABLE 3 DFT calculated parameters for the *cis*-Pt(II)

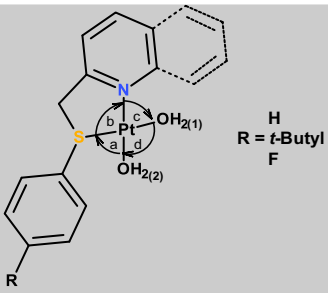

Property	Pt(L1)	Pt(L2)	Pt(L3)	Pt4[a]
MO energy (eV)				
LUMO	−3.27	−3.23	−3.30	−3.09
HOMO	−7.20	−7.19	−7.22	−7.09
$\Delta E_{L\text{-}H}$	3.93	3.96	3.92	4.00
NBO charges				
Pt	0.645	0.641	0.648	0.676
S	0.460	0.454	0.466	0.456
ω (eV)	6.97	6.85	7.06	6.48
Bond lengths (Å)				
d(Pt-$N_{qn/py}$)[b]	2.04	2.04	2.04	2.02
d(Pt-S)	2.40	2.39	2.40	2.41
d(Pt-$OH_{2\,(1)}$)	2.13	2.13	2.13	2.12
d(Pt-$OH_{2\,(2)}$)	2.11	2.10	2.10	2.11
Bond angle (°)				
S-Pt-$OH_{2\,(1)}$	174.8	172.9	175.1	176.6
$N_{qn/py}$-Pt-$OH_{2(2)}$	178.5	178.1	178.5	177.9
a	98.7	97.9	98.9	96.4
b	82.5	83.0	82.5	83.9

[a]Data from Mthiyane et al.[33]

[b]$N_{qn/py}$ = coordinated N-donor atom in the quinoline or pyridine ring.

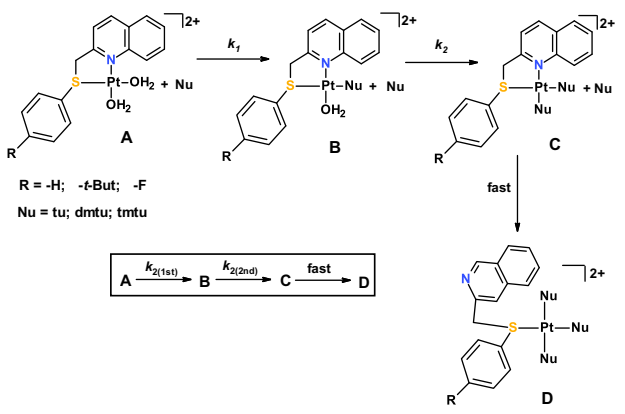

Scheme 2. Schematic representation of the two-step substitution of the aqua ligands from the Pt(II) complexes and the simultaneous decoordination of the N-end of the N,S ligand by entering thiourea nucleophiles (Nu = **tu**, **dmtu**, and **tmtu**) [Color figure can be viewed at wileyonlinelibrary.com]

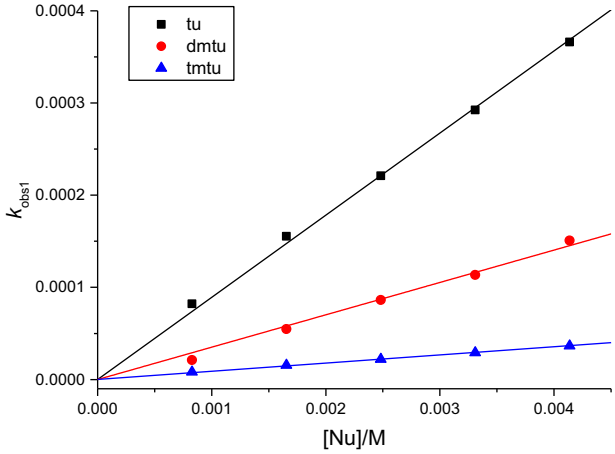

FIGURE 5 Plots of k_{obs1} versus [Nu] for the first substitutions steps of the reaction of 0.1 mM **Pt(L1)** at pH 2 (I = 0.1 M LiOTf/HOTf) and 25°C [Color figure can be viewed at wileyonlinelibrary.com]

The first substitution forms B, which reacts with a second nucleophile to form C, whose N-end of the N,S nonleaving ligand is simultaneously labilized by the trans coordinated thiourea nucleophile, facilitating the rapid coordination of a third thiourea nucleophile to produce D, for which four S atoms are coordinated to Pt(II) ion. This is also supported by data from Job's method of continuous variation of mole fraction of binary reactants on the absorbance of their solution in the complex formation reaction. This is illustrated in Figure 6.

Substitution of the aqua ligand trans to the thioether by thiourea nucleophiles, which is represented as step A → B was monitored on the stopped-flow reaction analyzer.

The second-order rate constants $k_{2(1st)}$ were determined from the slopes of the plots of $k_{obs.(1st)}$ versus [Nu], an example of the plot is shown in Figure 5.

The rate law for the substitution process can be expressed by Equation (1)[39,40]:

$$k_{obs(1/2)} = k_{2(1st/2nd)}[Nu] + k_{-1(1st/2nd)} \approx k_{2(1st/2nd)}[Nu] \quad (1)$$

where [Nu] = **tu**, **dmtu**, and **tmtu**.

The values of $k_{2(1st)}$ for the aqua substitution from the complexes by different nucleophiles are given in Table 4.

The second aqua substitution represented as B → C is ascribed to the substitution of the aqua ligand trans to the quinoline or pyridine moieties. The rate constant $k_{2(2nd)}$ for the second aqua substitution is calculated from the plot of $k_{obs.2nd}$ versus [Nu]. The substitution proceeds at a slower rate due to ligand shielding in the square plane upon coordination of the first thiourea nucleophile. The σ-inductive donation due to the coordinated thiourea nucleophile further increases the electron density onto the metal center making it less electrophilic. Combined, these factors result in the slower rate of substitution of the second aqua ligand.

TABLE 4 Rate constants $k_{2(1st/2nd)}$ for the consecutive substitution steps

	Nu	$k_{2(1st)}$ (M^{-1} s^{-1})	$k_{2(2nd)}$ (M^{-1} s^{-1})
Pt(L1) 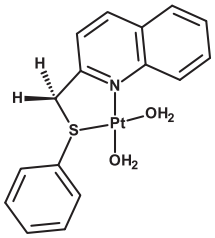	**tu**	21 ± 1	8.9 ± 0.3
	dmtu	13 ± 1	5.7 ± 0.3
	tmtu	9 ± 1	0.4 ± 0.1
Pt(L2) 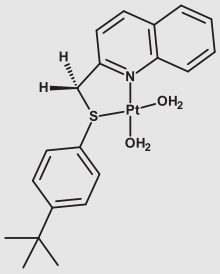	**tu**	335 ± 2	19.6 ± 0.1
	dmtu	254± 2	11.5 ± 0.2
	tmtu	86 ± 1	2.4 ± 0.1
Pt(L3) 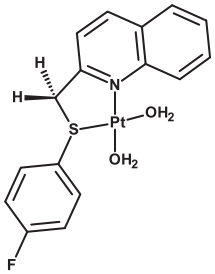	**tu**	287 ± 4	4.8 ± 0.1
	dmtu	155 ± 4	2.6 ± 0.1
	tmtu	59 ± 1	0.3 ± 0.1
Pt4[a] 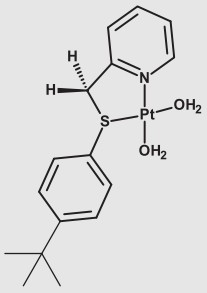	**tu**	4325 ± 16	24.3 ± 1.2
	dmtu	636 ± 11	17.2 ± 0.1
	tmtu	127 ± 2	6.6 ± 0.7

[a]Data from Mthiyane et al.[33]

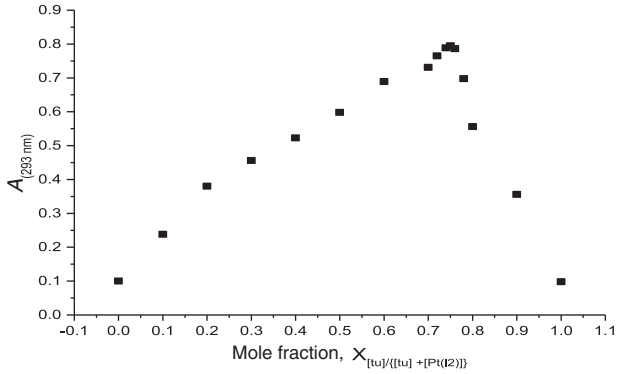

FIGURE 6 Job plot of absorbance values (at 293 nm) of solutions of **Pt(L2)Cl$_2$** (0.1 mM) and tu (0.1 mM) prepared in 0.1 M LiOTf/HOTf, pH 2 and at different mole fractions recorded after a 10-h aging period

3.5 | Job's method of continuous variation

A Job's plot (Figure 6)[41,42] was obtained from data presented in Figure SI 3 in the Supporting Information.

The absorbance for the reaction mixtures peak at an approximate tu mole fraction of 0.74, corresponding to complex formation product, **Pt(tu)$_3$** in which three tu ligands are coordinated to the metal center. This prompted us to propose a mechanism of substitution shown in Scheme, and which is similar to what has been previously proposed for the pyridyl-supported analogues.[33] The substitution of the second aqua ligand to form C triggers a rapid and simultaneous trans labilization of the N-end of the N,S nonleaving ligand by a third thiourea nucleophile, resulting in the PtS_4 species, D. Owing to the strong trans influence of the thiourea nucleophile coordinated trans to the quinolyl nitrogen, the Pt–N bond is weakened significantly, making it more susceptible to nucleophilic attack from a third thiourea nucleophile. A similar labilization effect on nitrogen-coordinated nonleaving ligands by thiourea has been reported before.[43] In a chloride substitution from a Pt(II) dinuclear complex linked by an ω,α-alkanediamine with NNN-non-leaving bridging head groups by **tu**, monitored by ^{195}Pt NMR spectroscopy, the final product of the substitution reaction was similarly a **PtS$_4$** species (as evidenced by new peak with a δ (^{195}Pt) in the range –3800 to –3900 ppm at the end of the reaction). Once the tu substituted the Cl leaving group, it labilized the trans N of the NNN-linked headgroups of the linker in a (rapid) very fast and not necessarily a rate-limiting step.

The temperature dependence of the second-order rate constants was regressed according to the Eyring equation (2)[44]:

$$\ln\left[k_{2(1st/2nd)}/T\right] = -\left(\Delta H^{\neq}{}_{1st/2nd}/R\right)(1/T) + \left[23.8 + \left(\Delta S^{\neq}{}_{1st/2nd}/R\right)\right] \quad (2)$$

Examples of the Eyring plots are shown in Figure 7 for the reactions of **Pt(L1)**.

The activation enthalpy ($\Delta H^{\neq}{}_{1st/2nd}$) and activation entropy ($\Delta S^{\neq}{}_{1st/2nd}$) were calculated from the slopes and y-intercepts of the Erying plots, respectively. The data are summarized in Table 5.

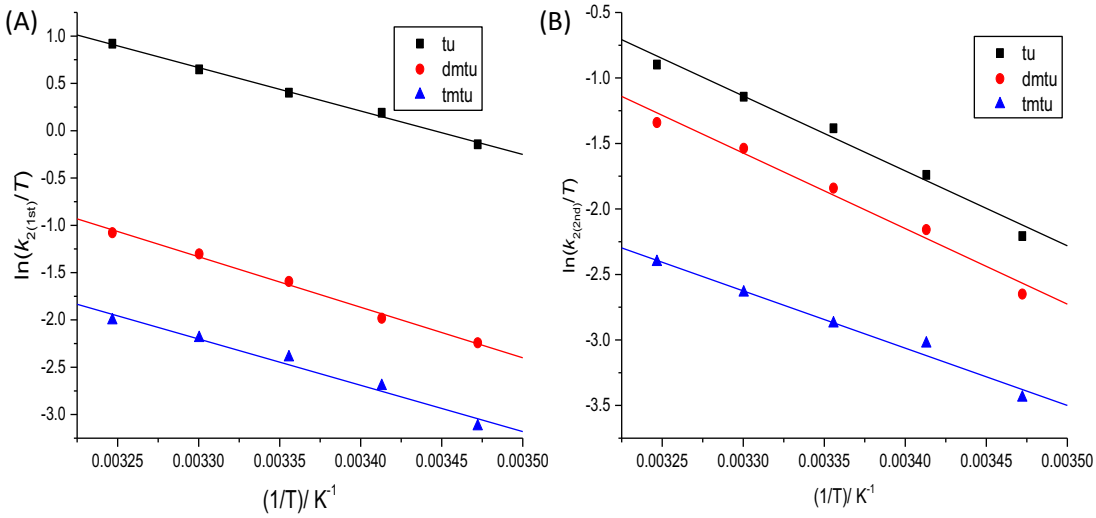

FIGURE 7 Eyring plots for (A) first and (B) second substitution steps for the reactions of 0.1 mM **Pt(L1)** and thiourea nucleophiles (6.1 mM), pH 2 (I = 0.1 M LiOTf/HOTf) [Color figure can be viewed at wileyonlinelibrary.com]

4 | DISCUSSION

The results in Table 4 indicate that the rate of substitution of the aqua leaving groups is sensitive to the nature of the substituents on the phenyl ring of the coordinated phenylthioether. The aqua ligand which is trans to the thioether group is substituted first. This is due to the strong σ-trans-directing ability of this moiety, which labilizes the Pt-$OH_{2(1)}$ bond trans to its position. The substitution of the first aqua ligand by thiourea as the entering nucleophile decreases in the following order: **Pt4 < Pt(L2) < Pt(L3) < Pt(L1)** and by factors of 204: 15: 14: and 1, respectively.

The strong positive σ-inductive donation of the *tert*-butyl substituent of **Pt(L2)** enhances the trans-directing ability of the thioether. This leads to an increased rate of substitution via the ground-state trans-influence when compared to the unsubstituted complex **Pt(L1)**, which has a weaker σ-donor capacity. Owing to the high diffusity of atomic orbitals of the S atom of the thioether, electron density can also be back donated into the low-energy lying antibonding molecular orbitals localized on the S atom thereby stabilizing the transition state during the substitution process. The π-acceptor capacity of the thioether is enhanced by the negative σ-inductive withdrawal of the fluorosubstituent for **Pt(L3)** and leads to an increase in the rate of substitution when compared to **Pt(L1)**. As a result, electron density is back donated from the filled *d*-orbitals of the Pt(II) ion of **Pt(L3)** into the empty but low-lying unoccupied orbitals of its thioether, resulting in a more electropositive metal center. Consequently, the formation of the bond with the entering thiourea nucleophiles stabilizes the transition state of the reactions of **Pt(L3)** relative to that of **Pt(L1)**. These observations are supported by the low pK_a values of the complexes, which are sensitive to the nature of the substituent on the phenyl para position. The electron-withdrawing substituents in **Pt(L3)** and **Pt(L1)** are capable of delocalizing electron density away from the Pt atom, making it more electrophilic. In contrast, the electron-donating *tert*-butyl substituent in **Pt(L2)** aids in the accumulation of electron density, resulting in an observed higher pK_a value.

Replacing the pyridine group with a quinoline ring results in a decrease in the rate of substitution of the aqua leaving groups. A comparison of the rate constants for **Pt4** and **Pt(L2)** demonstrates this fact. The decreased reactivity for **Pt(L2)** when compared to **Pt4** is due to a decreased π-back-donation into the quinolyl group orbitals, which increases electron density on the Pt atom. Similar trends have been reported previously.[18,19]

The second substitution of the aqua leaving group occurs trans to the quinoline moiety. Coordination of the first thiourea nucleophile imparts a steric shielding along the plane of the complex against nucleophilic attack from a second nucleophile. The steric hindrance due to the coordinated thiourea on the square-plane accounts for the slower substitution of the second aqua ligand. The reactivity factors for the substitution of the second aqua when thiourea is used as the entering nucleophile are 6: 5: 2: 1, and the order of reactivity of the complexes is **Pt4 < Pt(L2) < Pt(L3) < Pt(L1)**.

The nucleophilic character of thioureas at the Pt metal center resembles that of thiols (σ-donors) as well as thioethers (σ-donors/π-acceptors).[45] Consequently, the thiourea ligand trans to the coordinated quinoline or pyridine can potentially weaken the Pt–N bond trans to these moieties via its strong σ-donor character.[20] The labilization of the Pt–N bonds leads to the facile substitution of Pt–N bond of the N,S bidentate by a third thiourea nucleophile as outlined in Scheme 2 and Figure 7. However, the N,S bidentate of the ligand remains coordinated to the Pt(II) metal center through the S atom of the thioether. The inertness of the thioether toward

TABLE 5 Activation parameters for the consecutive substitution steps

	Nu	$\Delta H^{\neq}_{(1st)}$ (kJ mol^{-1})	$\Delta S^{\neq}_{(1st)}$ (J K^{-1} mol^{-1})	$\Delta H^{\neq}_{(2nd)}$ (kJ mol^{-1})	$\Delta S^{\neq}_{(2nd)}$ (J K^{-1} mol^{-1})
Pt(L1)	**tu**	44 ± 2	−63 ± 7	39 ± 1	−87 ± 3
	dmtu	38 ± 1	−66 ± 5	56 ± 2	−79 ± 5
	tmtu	41 ± 3	−86 ± 9	38 ± 4	−81 ± 10
Pt(L2)	**tu**	69 ± 3	−93 ± 8	56 ± 1	−89 ± 3
	dmtu	57 ± 2	−106 ± 6	49 ± 1	−96 ± 3
	tmtu	43 ± 2	−86 ± 7	38 ± 3	−81 ± 8
Pt(L3)	**tu**	53 ± 3	−28 ± 9	43 ± 2	−78 ± 6
	dmtu	53 ± 2	−28 ± 6	69 ± 3	−73 ± 8
	tmtu	40 ± 3	−79 ± 8	34 ± 2	−93 ± 6
Pt4[a]	**tu**	28 ± 1	−72 ± 4	36 ± 3	−100 ± 9
	dmtu	45 ± 2	−41 ± 6	47 ± 2	−63 ± 6
	tmtu	36 ± 1	−84 ± 4	37 ± 2	−177 ± 7

[a]Data from Mthiyane et al.[33]

trans-labilization by thiourea is levered by its strong σ-donor capacity.

The DFT calculations were undertaken to help support the observed trend in the substitution behavior of the complexes. For the quinolyl complexes, the theoretical DFT parameters namely electrophilicity indices (ω) and NBO charges indicate that the **Pt(L3)** complex is expected to have the highest reactivity due to its Pt atom being the most electrophilic. This somehow is contrasted by the reactivity trend observed experimentally, suggesting a σ-trans-effect as the dominating factor controlling the reactivity of the complexes. Owing to the stronger positive σ-inductive donation of the *tert*-butyl on the phenylthioether, there is more ground-state labilization of the trans bonded aqua ligand in **Pt(L2)** when compared to **Pt(L3)**. The reactivity of **Pt(L3)** is also influenced by the π-acceptor capacity of the thioether apart from the negative σ-inductive withdrawal of the fluoro group. This explains the high reactivity of **Pt(L2)** compared to **Pt(L3)**.

5 | CONCLUSIONS

The substitution of the first aqua ligand from three Pt(II) complexes bearing 2-(phenylthiomethyl)quinoline chelates is dependent upon the nature of the substituents on the thioether group and decreases in the order: **Pt4** < **Pt(L2)** < **Pt(L3)** < **Pt(L1)**. Both the electron-donating *tert*-butyl in **Pt(L2)** as well as electron-withdrawing fluoro group in **Pt(L3)** increase the rate of substitution when compared to **Pt(L1)**. Extending the comparison from **Pt(L2)** to **Pt4** reveals that replacing quinolyl moiety in the structure of nonleaving ligand pyridine increases the rate of substitution due to the relatively stronger π-acceptor property of the latter. The reactivity of the nucleophiles toward all the complexes decreases in the order: **tu** > **dmtu** > **tmtu**, which reflects the influence of their steric bulk. Low enthalpies of activation, negative entropies of activation, and dependence of rate on the concentration of the nucleophiles all support an associative mode of substitution of the labile ligands from the complexes.

ACKNOWLEDGMENTS

We thank the University of KwaZulu-Natal and the National Research Foundation of South Africa for financial support and a bursary to WMM.

ORCID

Allen Mambanda http://orcid.org/0000-0002-8113-3643

REFERENCES

1. Haviv F, DeNet RW, Michaels RJ, Ratajczyk JD, Carter GW, Young PR. 2-[(Phenylthio)methyl]pyridine derivatives: new antiinflammatory agents. *J Med Chem*. 1983;26:218–222.
2. Sadler PJ, Guo Z. Metal complexes in medicine: design and mechanism of action. *Pure Appl Chem*. 1998;70:863–871.
3. Muggia F, Bonetti A, Hoeschele J, Rozencweig M, Howell S. Platinum antitumor complexes: 50 years since Barnett Rosenberg's discovery. *Am J Clin Oncol*. 2015;33:4219–4226.
4. Bugarčić ŽD, Bogojeski J, van Eldik R. Kinetics, mechanism and equilibrium studies on the substitution reactions of Pd(II) in reference to Pt(II) complexes with bio-molecules. *Coord Chem Rev*. 2015;292:91–106.
5. Kosović M, Jaćimović, Bugarčić ŽD, Petrović B. Kinetics and mechanism of the substitution reactions of some monofunctional Pd(II) complexes with different nitrogen-donor heterocycles. *J Coord Chem*. 2015;68:3003–3012.
6. Wang D, Lippard SJ. Cellular processing of platinum anticancer drugs. *Nat Rev Drug Discov*. 2005;4:307–320.

7. Kelland L. The resurgence of platinum-based cancer chemotherapy. *Nat Rev Cancer*. 2007;7:573–584.
8. Bogojeski J, Volbeda J, Bugarčić ŽD, Freytag M, Tamm M. Platinum(II) complexes with hybrid amine imidazolin-2-imine ligands and their reactivity toward bio-molecules. *New J Chem*. 2016;40:4818–4825.
9. Summa N, Soldatović T, Dahlenburg L, Bugarčić ŽD, van Eldik R. The impact of different chelating leaving groups on the substitution kinetics of mononuclear PtII(1,2-trans-R,R-diaminocyclohexane)(X–Y) complexes. *J Biol Inorg Chem*. 2007;12:461–475.
10. Khusi BB, Mambanda A, Jaganyi D. The role of substituents in a bidentate N,N-chelating ligand on the substitution of aqua ligands from mononuclear Pt(II) complexes. *Transition Met Chem*. 2016;41:191–203.
11. Karmakar P. The effect of σ-donation on the interactions of cis-diaqua (2-aminomethylpiperidine)platinum(II) complex with biomolecules in aqueous medium: synthesis, kinetic and mechanistic study. *Transition Met Chem*. 2014;39:727–733.
12. Ray S, Karmakar P, Chattopadhyay A, Nandi D, Sarkar R, Ghosh AK. Kinetic and mechanistic investigations on some N,N-chelated Pt(II) oxalate complexes with some "S" containing biorelevant ligands at physiological condition. *Int J Chem Kinet*. 2016;48:347–357.
13. Jarzynka P, Topolski A, Uzarska M, Czajkowski R. New dinuclear platinum complexes. Synthesis and kinetics of chloride substitution by thiourea and glutathione in water–DMF solution. *Inorg Chim Acta*. 2014;413:60–67.
14. Hochreuther S, Nandibewoor ST, Puchta R, van Eldik R. Thermodynamic and kinetic behaviour of [Pt(2-methylthiomethylpyridine)$(OH2)_2]^{2+}$. *Dalton Trans*. 2012;41:512–522.
15. Samanta A, Ghosh GK, Mitra I, et al. Ligand substitution reaction on a platinum(II) complex with bio-relevant thiols: kinetics, mechanism and bioactivity in aqueous medium. *RSC Adv*. 2014;4:43516–43524.
16. Kosović M, Jovanović S, Bogdanović GA, et al. Kinetics and mechanism of the substitution reactions of some monofunctional Pt(II) complexes with heterocyclic nitrogen donor molecules. Crystal structure of $[Pt(bpma)(pzBr)]Cl_2 \cdot 2H_2O$. *J Coord Chem*. 2016;69:2819–2831.
17. Bellicini M, Cattalini L, Marangoni G, Pitteri B. Reactivity of neutral nitrogen donors in planar d8 metal complexes. Part 1. The system [1,2-bis(phenylsulfanyl)-ethane]dichloroplatinum(II) with pyridines in methanol. Effect of basicity and steric hindrance. *J Chem Soc, Dalton Trans*. 1994:1805–1811.
18. Ongoma P, Jaganyi D. The π-acceptor effect in the substitution reactions of tridentate N-donor ligand complexes of platinum(II): a detailed kinetic and mechanistic study. *Dalton Trans*. 2012;41:10724–10730.
19. Wekesa IM, Jaganyi D. The deleterious effect of pyrollic-nitrogen on the substitution reactivity of tridentate N^{C^N} platinum(II) complexes. *J Coord Chem*. 2016;69:389–403.
20. Basolo F, Pearson RG. *Mechanisms of Inorganic Reactions: A Study of Metal Complexes in Solution*. New York, NY: Wiley; 1967.
21. Tobe ML, Burgess J, *Inorganic Reaction Mechanisms*. Harlow, England: Longman; 1999.
22. Khusi BB, Mambanda A, Jaganyi D. Aqua substitution from mononuclear Pt(II) complexes with 2-(pyrazol-1-ylmethyl)quinoline non-leaving ligands. *J Coord Chem*. 2016;69:2121–2135.
23. Schiessl WC, Summa NK, Weber CF, et al. Experimental and theoretical approaches to the protonation of thiourea: a convenient nucleophile in coordination chemistry revisited. *Z Anorg Chem*. 2005;631:2812–2819.
24. Malachowski MR, Adams M, Elia N, Rheingold AL, Kelly RS. Enforcing geometrical constraints on metal complexes using biphenyl-based ligands: spontaneous reduction of copper(II) by sulfur-containing ligands. *J Chem Soc, Dalton Trans*. 1999:2177–2182.
25. Malachowski MR, Adams ME, Murray D, et al. Copper(II) complexes of bidentate ligands containing nitrogen and sulfur donors: synthesis, structures, electrochemistry and catalytic properties. *Inorg Chim Acta*. 2009;362:1247–1252.
26. Rauterkus MJ, Fakih S, Mock C, Puscasu I, Krebs B. Cisplatin analogues with 2,2′-dipyridylamine ligands and their reactions with DNA model nucleobases. *Inorg Chim Acta*. 2003;350:355–365.
27. Bugarčić ŽD, Petrović BV, Jelić R. Hydrolysis of $[Pt(dien)H_2O]^{2+}$ and $[Pd(dien)H_2O]^{2+}$ complexes in water. *Transition Met Chem*. 2001;26:668–671.
28. Origin 7.5TM SRO, v7.5714 (B5714). Northamption, MA: Origin Lab Corporation; 2003.
29. Becke AD. Density functional thermochemistry. III. The role of exact exchange. *J Chem Phys*. 1993;98:5648–5652.
30. Lee C, Yang W, Parr RG. Development of the Colle-Salvetti correlation-energy formula into a functional of the electron density. *Phys Rev B*. 1988;37:785–789.
31. Hay PJ, Wadt WR. Ab initio effective core potentials for molecular calculations. Potentials for K to Au including the outermost core orbitals. *J Chem Phys*. 1985;82:299–310.
32. Frisch MJ, Trucks GW, Schlegel HB, et al. Gaussian 09, Revision A.I. Wallingford CT: Gaussian; 2009.
33. Mthiyane WM, Mambanda A, Jaganyi D. Substitution of aqua ligands from cisplatinum(II) complexes bearing 2-(phenylthiomethyl)pyridine spectator ligands. *Transition Met Chem*. 2017;42:739–751.
34. Bruker APEX2, SAINT and SADABS. Madison, WI: Bruker AXS; 2010.
35. Sheldrick G. A short history of SHELX. *Acta Crystallogr Sect A Found Crystallogr*. 2008;64:112–122.
36. Kinunda G, Jaganyi D. A kinetic study of aqua ligand substitution in dinuclear Pt(II) complexes containing four non-coplanar pyridine ligands. *Transition Met Chem*. 2014;39:451–459.
37. Mambanda A, Jaganyi D, Hochreuther S, van Eldik R. Tuning the reactivity of chelated dinuclear Pt(II) complexes through a flexible diamine linker. A detailed kinetic and mechanistic study. *Dalton Trans*. 2010;39:3595–3608.
38. Mambanda A, Jaganyi D. Understanding the role of the flexible bridging linker through kinetics and mechanistic study of Pt(II)

amphiphiles derived from a bis(2-pyridylmethyl)amine chelate head group. *Dalton Trans*. 2012;41:908–920.

39. Atwood JD. *Inorganic and Organometallic Reaction Mechanisms*. New York, NY: Wiley-VCH; 1997.
40. Asperger S. *Chemical Kinetics and inorganic Reaction Mechanisms*. New York, NY: Kluwer Academic/Plenum Publishers; 2003.
41. Hill ZD, MacCarthy P. Novel approach to Job's method: an undergraduate experiment. *J Chem Educ*. 1986;63:162.
42. Job P. Formation and stability of inorganic complexes in solution. *Ann Chim Appl*. 1928;9:113–203.
43. Erturk H, Maigut J, Puchta R, van Eldik R. Substitution behaviour of amine-bridged dinuclear Pt(II) complexes with bio-relevant nucleophiles. *Dalton Trans*. 2008:2759–2766.
44. Jordan RB. *Reaction Mechanisms of Inorganic and Organometallic Systems*. New York, NY: Oxford University Press; 1991.
45. Cattalini L, Orio A, Doni A. Reactivity of amines toward a neutral platinum(II) complex. *Inorg Chem*. 1966;5:1517–1519.

SUPPORTING INFORMATION

Additional supporting information may be found online in the Supporting Information section at the end of the article.

How to cite this article: Mthiyane WM, Mambanda A, Jaganyi D. Reactivity of *cis*-platinum(II) complexes with 2-(4-substituted)phenylthiomethyl)quinoline non-leaving ligands toward thiourea nucleophiles. *Int J Chem Kinet*. 2018;50:531–543. https://doi.org/10.1002/kin.21178